AI Based Reference Signal Generation for Renewable Source and Energy Storage Incorporated Multilevel UPQC

Guguloth Mohan Babu[*‡], G. Suresh Babu[**], Gummadi Srinivasa Rao[***], K. Ramya[****], NMG Kumar [*****], Ramprasad Vangalapudi[******], B. Pavan Kumar[******], N. Vasantha Gowri[**], Saroj Pradhan[******]

*Department of Electrical Engineering, Osmania University, Hyderabad, Telangana, India.

**Department of Electrical and Electronics Engineering, Chaitanya Bharathi Institute of Technology, Telangana

*** Department of Electrical and Electronic Engineering, Velagapudi Ramakrishna Siddhartha Engineering College, Siddhartha Academy of Higher Education (Deemed to be University) Kanuru, Vijayawada, Andhra Pradesh, India

**** Department of Electrical and Electronics Engineering, SreeVahini Institute of Science and Technology, Tiruvuru, India

*****Department of Electrical and Electronics Engineering, SreeVidyanikethan College of Engineering, Tirupathi, India

****** Department of Electrical and Electronics Engineering, Sreenidhi Institute of Science and Technology, Hyderabad, India, 501301

****** Department of Electrical Engineering, PMEC, Berhampur, India

(mohanbabuguguloth1985@gmail.com, gsureshbabu_eee@cbit.ac.in, vasu1in@vrsiddhartha.ac.in, nmgkumar@gmail.com, ramprasadgurukul@gmail.com, pavankumarb@sreenidhi.edu.in, vasanthagowri_eee@cbit.ac.in, saroj.ee@pmec.ac.in)

‡Corresponding Author: Guguloth Mohan Babu, Department of Electrical Engineering, Osmania University, Hyderabad, Telangana, India, Tel: +91-8328180776, mohanbabuguguloth1985@gmail.com

Received: 10.09.2023 Accepted:28.10.2023

Abstract: This study examines the photovoltaic (PV), and battery energy storage (BES) associated diode clamped five-level unified power quality conditioner (5L-UPQC) to handle the power quality (PQ) related problems. To eliminate the requirement of the complex transformations like abc, dq0, αβ , the (Artificial neural network) ANN-based control scheme with LMBP training method is adopted for the 5L-UPQC to supply the necessary reference signals for the (Voltage source converters) VSC's. The hybrid controller combines both ANN and (Sliding mode controller) SMC is adopted for DC link balancing. The prime goal of the developed scheme is to maintain DC link capacitor voltage (DLCV) during load changes and decrease supply current and load voltage Total harmonic distortion (THD). In addition, the source voltage fluctuations like sag, disturbance and swell were eliminated. The suggested method was demonstrated on two cases with several permutations of loads. However, the comparison is carried out with the proportional integral controller (PIC), SMC and ANN to reveal the working of the suggested technique. The developed model is executed on the MATLAB/ Simulink platform.

Keywords Power quality, unified power quality conditioner, artificial neural network, total harmonic distortion, solar system.

Nomenclature:

UPQC	Unified Power Quality Conditioner
Five-level-UPQC	5L-UPQC
PV	Photovoltaic
BSS	Battery Storage System
PQ	Power Quality
SRF	Synchronous Reference Frame Theory
p-q	Instantaneous Reactive Power Theory
ANN	Artificial Neural Network
LMBP	Levenberg- Marquardt Back Propagation

DLCV	Direct Current Link Capacitor Voltage
THD	Total Harmonic Distortion
PF	Power Factor
GA	Genetic Algorithm
PSO	Particle Swarm Optimization
PIC	Proportional Integral Controller
SHAPF	Shunt Active Power Filter
GWO	Grey Wolf Optimization
PWM	Pulse Width Modulation
MSE	Mean Square Error
SMC	Sliding Mode Control
FLC	Fuzzy Logic Controller
VSC	Voltage Source Converter
BBO	Biogeography Based Optimization
SEAF	Series Active Power Filter
ACO	Ant Colony Algorithm
FOPID	Fractional Order Proportional Integral Derivate
MSF	Member Ship Function
ANFIS	Artificial Neuro-Fuzzy Interface System
FF-ANN	Firefly Based ANN
PPFFA	Predator-Prey Firefly Algorithm
SPG	Solar Power Generation
V_{LL}	Line to Line RMS Voltage
CE	Change In Error
BC	Boost Converter
OL	Output Layer of ANN
IL	Input Layer of ANN
HL	Hidden Layer of ANN
BBC	Buck Boost Converter
E	Error
V_{l_abc}	Voltage at Load end in abc Phases
m	Modulation Index
$V_{cr,pp}$	Peak-to-Peak Voltage Ripple
Δi_{lmax}	Peak Ripple Current
V_m	Peak Voltage of The System
a_f	Over Loading Factor
V_{se_abc}	Series Filter Supplied Voltage In abc Phases
f_{sh} f_{se}	Switching Frequency
$V^{ref}{}_{se\_abc}$	Reference Series Injected Voltage for Phases abc
L_{se}	SEAF Inductance
V_{S_abc}	Source Voltage For abc Phases
R_S , L_S	Grid Resistance and Inductance
C_{dc}	Capacitance of DC link
R_{sh}	SHAPF Resistance
V_{dc}	Voltage across DC link capacitor
$V^{ref}{}_{dc}$	Reference DLCV
Δi_{dc}	DCLink Output Error
$i^{ref}{}_{dc}$	The reference value of DC Current
R_{se}	SEAF Resistance
i_{l_abc}	Current at Load End in abc Phases
$V_{dc,err}$	DLCV Error
i_{S_abc}	Grid Source Current in abc Phases
$i^{ref}{}_{BS}$	Battery Reference Current
i_{ph}	Photo Current Source
$i_{BS,err}$	Error Current Received from Battery
L_{sh}	Shunt VSC Inductance
i_d	Forward Diode Carrying Current
$R_{s,PV}$ and $R_{sh,PV}$	Series and Parallel Cell Resistances of PV
$i^{ref}{}_{sh\_abc}$	Shunt Reference Current in abc Phases
$i_{sh,PV}$	Parallel Current of PV Cell
i_{sh_abc}	Shunt Current in abc Phase
i_{PV}	PV Cell Output Current
i_{rs}	Reverse Saturation Current
i_{sc}	Short Circuit Current
q	Electron Charge

$i_{BS,er}^{*}$	Reference Error Current Chosen For The Battery
η	Diode Ideal Factor
k	Boltzmann's Constant
T	Cell Temperature
N_p, N_s	Number Of Parallel And Series Connected PV Cell
G	Solar Irradiance (W/M^2) and At STC
T_n	Nominal Temperature
E_g	Band Gap of Semi Conductor
P_{PV}	Output PV Power
P_{BS}	Battery Output Power
P_{dc}	Power at DC Link
E_0	No-Load Battery Voltage
$V_{b,charge,\ b\_discharge}$	Battery Charge Discharge Voltage
R	Internal Resistance of Battery
i_b	Battery Current
E_0	Battery Constant Voltage
K	Polarization Constant
$SOCOB$	State of Charge of Battery

1. Introduction

In recent years, integrating renewable energy systems like solar and wind into the distribution network has been encouraged to reduce the stress on converters and ratings. The performance of wind systems connected to UPQC was studied on different loads and faulty conditions by adopting hysteresis and PWM techniques [1]. Next, the PSO in association with the GWO-based optimization algorithm, was chosen to obtain the suitable FOPIDC controller parameters of SHAPF for compensating the reactive power while minimizing THD for the balanced and unbalanced loads as the case studies with an experimental investigation [2]. Besides, a new hybrid enhanced EGO associated with the ANN technique for the SHAPF was introduced to reduce the current signal's distortions and improve the distribution network PQ [3]. Further, the power flow analysis of the UPQC was studied on a three-phase distribution system with various faculty conditions from the point of impedance matching technique [4]. The UPQC incorporated with the solar system was developed to address PQ issues efficiently. In addition, a novel fuzzy-based PIC was suggested for the MPPT to extract maximum power and balance DLCV [5].

However, to reduce the complexity, the ANN was considered for UPQC reference signal generation to solve PQ issues [6]. The self-tuning filter-based method was developed for UPQC integrated with renewable sources to address PQ issues [7]. The various existing algorithms for controlling the operation of SHAPF and harmonics isolation techniques, DLCV regulation, and current control methods are discussed [8].The intelligent fuzzy-tuned proportional integral controller PIC was designed for the hybrid shunt active and passive filters to minimize the current THD. However, the performance analysis was carried out for varying loads using Clarke's transformation [9]. Meanwhile, by adopting ANN, the Solar PV powered UPQC was presented to reduce grid current THD during voltage fluctuations like sag, swell. In addition, the proposed method was compared with SRF and reactive power theory methods under varying load conditions [10].

Besides, the microgrid-connected multilevel DSTATCOM was developed to eliminate voltage and current distortions effectively [11]. A novel load equivalence conductance technique has been introduced to the UPQC to improve PQ and to regulate energy transfer between sources and loads [12]. Further, to control and to handle DLCV feed forward, ANN has been suggested for PV in combination with the wind associated with UPQC [13]. The H bridge inverter-based single-phase SHAPF with a modified Predictive Current Control method was introduced to reduce THD in grid current waveform [14].Besides, a comprehensive study was done on phase synchronization methods used to handle the performance of SHAPF [15].

However, the GWO was suggested for the optimal gain parameters selection of PIC-based UPQC to reduce harmonics for three-phase linear and non-linear loads [16]. The hybrid fuzzy ANN-based control technique was adopted for UPQC to diminish current THD and voltage fluctuations and advance network usage [17]. A biogeography-based optimization (BBO) algorithm was selected to obtain optimal gain values of PIC and for fast action in fault identification with higher accuracy with a motive of stabilizing DLCV fluctuations [18]. Intelligent hybrid controllers like fuzzy-PIC and fuzzy proportional integral derivative controllers were proposed for the AC-DC micro-grid system to enhance voltage stability and handle PQ during the presence of D-STATCOM [19]. A PIC was adopted to stabilize the DLCV for SHAPF to successfully address PQ problems by adopting hysteresis current control for pulse generation. Additionally, performance was studied on both linear and non-linear loads [20].

ACO was chosen for selecting the gain parameters of PI controller for the SHAPF to reduce THD under several loading conditions [21]. However, a Soccer match optimization was chosen for the ANNC bias and weights selection for the solar battery linked UPQC [22]. The FLC was developed for SEAF of the distribution network to minimize the current and voltage-related PQ problems [23]. The predator-prey firefly algorithm was selected for the optimal selection of gain parameters of PIC adapted to the SHAPF to reduce the THD and to enhance the PF [24]. The Improved Bat and Moth Flame metaheuristic optimization methods were hybridized to solve the PQ issues by selecting the gain values of PIC [25].

The hybrid control technique with both characteristics of FLC and ANN was recommended to UPQC for reducing the imperfections and distortions at grid voltage and source current with DLCV balancing for dynamic loads [26]. The metaheuristic firefly nature-inspired algorithm was used to

train ANNC and was developed for the shunt VSC for the PV/ battery UPQC to reduce the MSE and minimize THD [27]. A soccer league optimization was proposed to select PIC gain parameters for UPQC to successfully handle both voltage fluctuations and current distortions [28]. The ANN-based method was suggested for 5L-UPQC to minimize THD and suppress voltage distortions [29]. An adaptive hysteresis band with FL-C was implemented to the PV-associated 9-level VSC-based UPQC to obtain fluctuations-free voltage waveforms [30]. The LMBP-trained ANN controller was adopted for UPQC to solve the grid voltage and current problems successfully [31]. It was investigated [32] the advantages and difficulties of integrating renewable energy sources into the system and their control strategies. A few recommendations were also made to transform the conventional grid into a smart grid, and the implications of smart grid technologies on the national grid were underlined [33]. For changes in solar irradiation, the comparison of P & O and PSO algorithms to provide MPP for the PV system was investigated [34]. Integration of renewable sources to micro grid for MPPT was studies with power management [35]. High voltage isolated ACDC converters were developed based on the modular technology [36]. Fuzzy logic controller was suggested for PV-MPPT to improve the overall performance by maximum power point tracking [37]. The optimal controllers were designed for the FACTS devices to address PQ issues. [38-41]

It is clear from most literature publications that they primarily concentrated on various controllers using the pre-existing traditional methods for UPQC that included complicated transformations. This publication presents an ANN-based reference signal-generating method for PV/battery-coupled DC link UPQC. The prime contribution of this work is as follows:

- The LMBP training-based ANNC is proposed to produce effective reference signals to avoid the requirement of traditional abc-dq0-αβ0 conversions.
- The hybrid controller combination of ANN with SMC properties is developed for DC Link balancing.
- The prime goal of the suggested scheme is to diminish the source current THD, improve the power factor, and eliminate grid voltage side troubles like (disturbance, swell, sag, etc.)
- The solar PV and battery systems are coupled to the DC link of 5L-UPQC via boost and buck-boost converter to meet the load demand, maintain stable DLCV at load variations, and minimize stress and burden on VSC.
- In addition, the suggested ANNC for 5L-UPQC in association with the PV and battery energy storage (5L-UPVBES) is examined on two test cases for different loading conditions to show its superior performance concerning the minimization of current waveform THD and voltage waveform fluctuations.
- The performance was tested by comparing it with PIC and SMC techniques. Table 1 gives the state-of-the-art and literature review. This paper is aligned as follows: section 2 provides the modelling of 5L-UPVBES, Section 3 explains the proposed ANN control scheme, Section 4 demonstrates the results and discussion, and Section 5 concludes the manuscript.

2. Modelling of Developed5L-UPVBES

Figure 1 depicts the proposed 5L-UPVBES arrangement, in which the PV and batteries are connected to the UPQC's DC link. The UPQC is a single device that combines the functions of series and shunt filters. The SAPF seeks to address grid-side voltage difficulties by giving the appropriate compensating voltage V_{se}via inductor L_{se}through the injecting transformer. Similarly, the SHAPF is linked to the grid via the interface inductance L_{sh}. By injecting suitable compensating current (i_{sh}), the SHAPF strives to eliminate current waveform harmonics and maintain DLCV (V_{dc}) steady with minimal settling time.

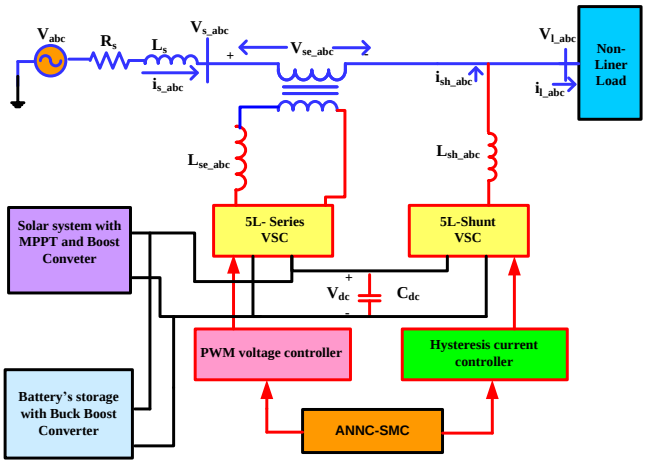

Fig. 1. Proposed 5L-UPVBES configuration.

Table 1: A literature survey (current start of art)

Ref/ year	Control		PQ Issues				Loads	
[No]/Year	Reference signal generation	Controller	THD	DLCV balancing	Supply Voltage sag, swell	Supply Voltage disturbance	Non-linear sensitive load	Unbalanced load
[2] / 2020	p-q theory	FOPID	✓				✓	✓
[1]/ 2022	SRF	PIC	✓					
[6]/ 2023	ANN	ANN	✓	✓	✓	✓	✓	✓
[9]/ 2022	SRF	FUZZY-PI	✓	✓			✓	

[13]/ 2021	ANN	ANN	✓			✓		✓	✓
[18]/ 2021	SRF	PI-BBO	✓			✓		✓	✓
[25]/2021	SRF	ANFIS	✓					✓	✓
[23]/2018	p-q	FUZZY	✓			✓		✓	
[24]/ 2019	SRF	PPFFA	✓					✓	✓
[21]/2019	SRF	PI-ACO	✓					✓	✓
[29]/ 2017	ANN	ANN	✓	✓		✓		✓	✓
[27]/2023	SRF	FF-ANN	✓	✓		✓	✓	✓	✓
Proposed 5L-UPVBES	**ANNC**	**ANN-SMC**	✓	✓		✓	✓	✓	✓

The most common multilevel topology is the diode-clamped inverter, in which the output voltage is modulated by clamping the dc bus voltage using a diode as the clamping device. The fundamental concept underlying this inverter is using diodes to reduce the voltage stress on the electrical equipment. The voltage across each capacitor and switch is known as V_{dc}. A n-level converter requires (n-1)*(n-2) diodes, (n-1) voltage sources and (2n-1) switching components. However, with the increase in the levels, the output quality is improved and becomes closer to sinusoidal. A 5L diode clamped for a single phase is shown in Figure 2. Table 2 lists the 5L diode clamped switching order.

2.1. Selection of C_{dc} and V_{dc}

From [29], under faulty conditions, assume the shunt and series VSC's power handling capacities are 0.5XkVA and 2XkVA, respectively. The kVA rating of VSC and V_{dc} is inversely proportional. By the change of 25% of V_{dc}, the equivalent change in the energy across C_{dc} is calculated by Eq. (1)

$$\Delta E_{dc} = 1/2C_{dc}[(1.125V_{dc})^2 - (0.875V_{dc})^2] \quad (1)$$

Assume that for the suppose the load changes from 2XkVA to 0.5XkVA in 'n' cycles in 'T' sec, then the corresponding change in the system's energy is given by

$$\Delta E_s = (2X - X/2)n.T \quad (2)$$

By, equating Eq. (1) and (2), the C_{dc} is given by Eq. (3)

$$C_{dc} = \frac{2(2X - X/2)n.T}{(1.125V_{dc})^2 - (0.875V_{dc})^2} \quad (3)$$

Let, V_{dc} is m times to V_m. Where, 'm' modulation index varies between 1.2 and 2. However, %THD depends on L_{sh} and V_{dc} so the value of m is selected as 1.6 [29] for minimum THD. Therefore, $V_{dc}$is given by Eq. (4)

$$V_{dc} = 1.6 * V_m \quad (4)$$

The V_{dc} for n level converter is evaluated by using [29] Eq. (5)

$$V^{ref}{}_{dc} = V_{dc}/(n-1) \quad (5)$$

2.2. Selection of Coupling Inductor for Shunt and Series VSC

The coupling inductors adopted to connect the series and shunt VSC's to the source and the load are limited by di/dt and magnitude of currents. The Δi_{lmax} occurs at m=0.5, given in Eq. (6) is controlled by PWM [29].

$$\Delta i_{l\max} = V_{dc}/6 f_{sw} L_{se} \quad (6)$$

Assuming the ripple current is about 10% of the maximum peak-to-peak current given by Eq. (7)

$$\Delta i_{l\max} = 0.1 * i_{\max} \quad (7)$$

Therefore, the maximum current handling by a series capacitor in terms of power and phase voltage is given by Eq. (8). By using Eq. (6) and (8) L_{se} can be calculated.

$$i_{\max} = \frac{\sqrt{2} * P_r}{3 * V_{ph}} \quad (8)$$

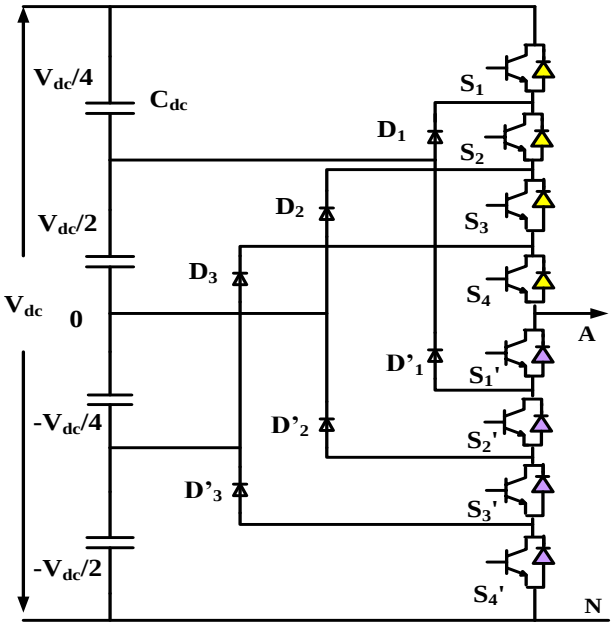

Fig. 2. 5L Diode clamped single phase.

By heuristically testing [29] it has been identified that for m=1.6, $V^{ref}{}_{dc}$= 700, and L_{sh}= 15 mH the % THD is lower. The value of L_{sh} is given by Eq. (9)

$$i_{\max} = \frac{V_{dc}}{4.h.f_{sw\max}} \quad (9)$$

Where, h is the hysteresis band 5-10%.

Table 2. Switches ON/OFF for 5L diode clamped UPQC

V_{AN}	S1	S2	S3	S4	S'1	S'2	S'3	S'4
$V_{dc}/2$	ON	ON	ON	ON	OFF	OFF	OFF	OFF
$V_{dc}/4$	OFF	ON	ON	ON	ON	OFF	OFF	OFF
0	OFF	OFF	ON	ON	ON	ON	OFF	OFF
$-V_{dc}/4$	OFF	OFF	OFF	ON	ON	ON	ON	OFF
$-V_{dc}/2$	OFF	OFF	OFF	OFF	ON	ON	ON	ON

2.3. Modelling of External Support of 5L-UPQC

The solar/battery-fed DC link is proposed for the diode clamped 5L-UPQC. It consists of a hybrid solar and battery energy system to regulate the DLCV during the variation in loads. External support can reduce the converter ratings and stress by lowering the utility's demands. The equation for DC link power demand (P_{dc}) of the suggested technique is given in equation (10).

$$P_{PV} + P_{BSS} - P_{dc} = 0 \quad (10)$$

2.3.1. *Solar power generation system (SPG)*

In this work, PV model is taken from the Simulink library. The PV models are connected in series to form a string, and some of such strings are connected in parallel to generate the required amount of voltage and current. Every PV cell is modelled in the module using a single diode equivalent circuit [31] as shown in Fig 2. It consists of photo current source (i_{ph}) with forward diode carrying current (i_d), a series and parallel cell resistances ($R_{s,PV}$ and $R_{sh,PV}$) carrying current of (i_{PV}, $i_{sh,PV}$). The PV cell identifies sun irradiation and converts it into current. Practically, PV cells are aligned in groups in larger number called PV modules. However, these modules are connected in series or parallel depending on the requirement to create PV arrays which are used to generate electricity in PV generation systems. PV module photo current source (i_{ph}) is obtained by Eq. (11) and PV module reverse saturation current i_{rs} is given by Eq. (12)

$$i_{ph} = [i_{SC} + K_i(T - 298)] * G / 1000 \quad (11)$$

$$i_{rs} = i_{SC} / [\exp(qV_{oc} / N_s \eta kT) - 1] \quad (12)$$

Here, i_{SC} is the short circuit current, K_i is i^{th} cell short circuited current, q is the electron charge, η is the diode ideal factor, k Boltzmann's constant and T denotes the cell temperature, G is the solar irradiation, $V_{oc}$is the open circuit voltage and N_s, N_p are the series and parallel connected PV cells to form module.

The module saturation current depends on cell temperature which is given by Eq. (13) and output current of module is given by Eq. (14).

$$i_{mo} = i_{rs}[T / T_n]^3 \exp[q * E_g / \eta k(1/T - 1/T_n)] \quad (13)$$

$$i_{PV} = N_p * i_{ph} - N_p * i_{mo} * [\exp(V_{pv} / N_s + i_{PV} * (R_{s,PV}) / \eta V_t) - 1] - i_{sh,PV} \quad (14)$$

Where,

$$V_t = k * T / q$$
$$i_{sh,PV} = V_{PV} * ((N_p / N_s) + i_{PV} * R_{s,PV}) / R_{sh,PV} \quad (15)$$

Here, T_n is the nominal temperature, $E_g$is the band gap of semi conductor. The output power obtained by the solar system (P_{PV}) is calculated by equation (16). The solar cell characteristics for constant temperature and variable irradiation is exhibited in Figure 3

$$P_{PV} = V_{PV} \times i_{PV} \quad (16)$$

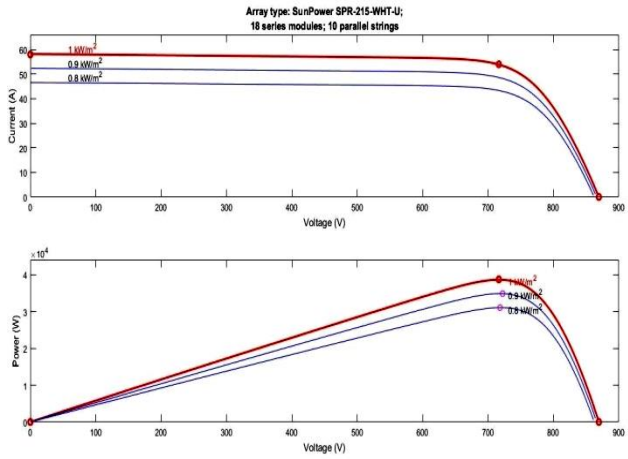

Fig. 3. PV cell characteristics at various irradiation and constant temperature 25°C..

2.3.2. Battery storage system (BSS)

The BSS provides support in stabilizing the DLCV. Battery consists of cells arranged in series or parallel to achieve the desired voltage and current. This work selects Li-ion batteries from the Simuink library due to its advantages like slow discharge and low maintenance cost. The charging/discharging model of the Li-ion battery is in Eq. (17)

$$V_b = V_{b\_charge,b\_discharge}(i_t, i^*, i_b) - i_b R \quad (17)$$

Where, $V_{b\_charge,b\_discharge}$ is the battery charge and discharge voltage, R is the internal battery resistance, $i_b$battery current. The charge and discharge of Li-ion type battery is expressed in terms of constant voltage E_0(Volts) , R internal resistance and battery capacity Q, K is the polarization constant given by Eq. (18).

$$E_{b\_charge} = E_0 - K(\frac{Q}{0.1Q + i_t})i^* - K(\frac{Q}{Q - \int i_t dt})i_t + Ae^{-b^* i_t} - i_b * R \quad (18)$$

$$E_{b\_discharge} = E_0 - K(\frac{Q}{Q + i_t})i^* - K(\frac{Q}{Q - \int i_t dt})i_t + Ae^{-b^* i_t} - i_b * R$$

The state of charge of battery (*SOCOB*) is expressed in Eq (19).

$$SOCOB = 50(1 + \int i_{BSS}\ dtQ) \quad (19)$$

The SPG will decide whether the battery to charge or discharge while satisfying the constraints given by Eq. (20). The discharge of the battery is shown in Figure 4. The rating selected for solar and battery systems are listed in Table 3. Figure 5 gives the control system for external supply sources.

$$SOCOB_{\min} \le SOCOB \le SOCOB_{\max} \quad (20)$$

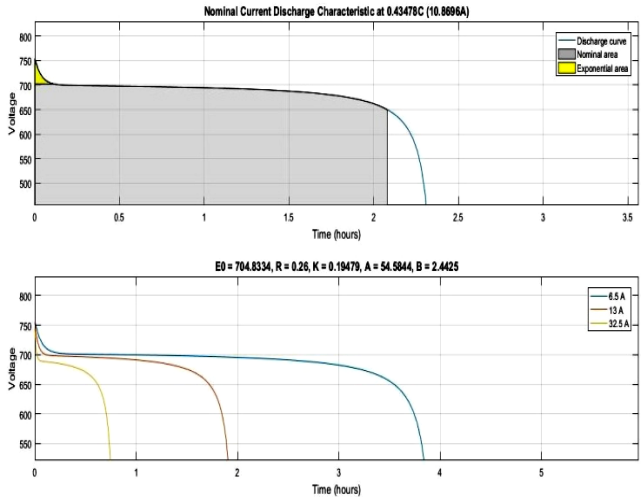

Fig. 4. Li-ion battery characteristics for discharge.

Table 3. Solar and BSS Ratings

Equipment	Factor	Value chosen
PV single panel (Sun power SPR-215-WHT-U)	Rated Power	214.92W
	Open circuit voltage	39.8V
	Short circuit current	5.8A
	Under max power the voltage & current	39.8V /5.4A
	Number of PV cells assembled in parallel, series	11, 18
Li-ion battery	Rated Capacity of battery	25Ah
	Normal Voltage	650V
	Fully charge voltage	756.59V
	Cut off voltage	487 V

3. Proposed Control Scheme for 5L-UPVBES

In general, V_{dc}changes when the distribution side's dynamic load varies. However, to restore normalcy to the system, Vdc must be reset to its previous value for a brief period. With the recommended ANNC, the PWM approach generates gate pulses.

3.1. Shunt VSC with Hybrid Controller

The primary goal of SHAPF is to remove flaws in the current signal and stabilize DLCV over faults and variable loading circumstances by introducing compensating currents.

3.1.1. ANN controller

ANN's structure includes an OL, an IL, and an HL. Where the IL gathers data from the input and sends it to HL; later, it is multiplied by the corresponding weights on the linked links, which are joined between the IL and HL. Here, calculations are performed with a predetermined bias on HL, and the outcomes are gathered in OL.

The LMBP-based ANN is chosen in this case. The connection weights are changed in training by assessing the error to achieve the desired output. For ANN training, where the performance function is MSE, the LMBP training technique is used. The LMBP algorithm uses the generated derivatives for weight update, which has the advantages of efficient learning and rapid convergence [32]. As illustrated in Fig. 6, the ANN controller created for DLCV balancing has one input and one output with a single hidden layer of 100 neurons.

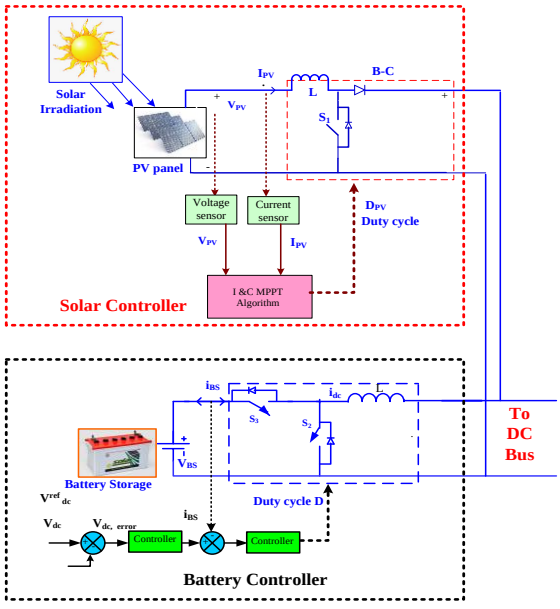

Fig. 5. Control system for external supply sources.

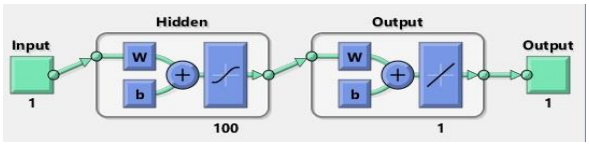

Fig. 6. Structure of ANNC for DClink balancing.

In multilayer perceptron networks, each neuron poses summation and activation functions. However, these neurons among the layers are interconnected with some numerical weights shown in Fig 7. The role of the summation function is to add the bias with the multiplication of inputs with weights as given in Eq. (21). Where β_k is a bias w_{pk} is the weight joining *p* to *k* neuron and m inputs. In general, for nonlinearity, the sigmoid function is considered as activation function shown by Eq. (22). Hence, the *k* neuron output is exhibited [24] in Eq. (23).

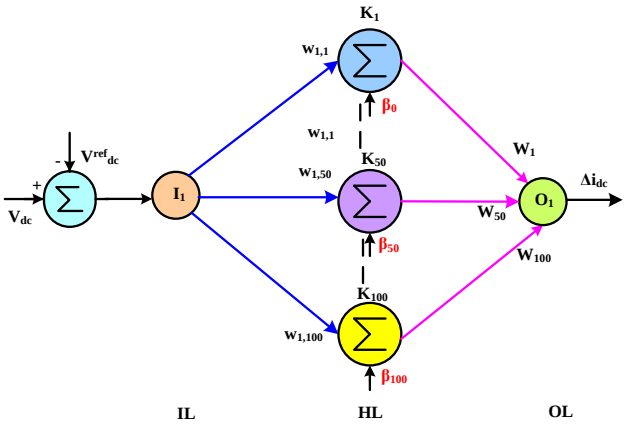

Fig. 7. MLP for ANNC for DC link balancing.

$$S_k = \sum_{p=1}^{m} w_{p_k} I_p + \beta_k \quad (21)$$

$$f(x) = \frac{1}{1+e^{-x}} \quad (22)$$

$$O_k = f_k\left(\sum_{p=1}^{m} w_{p_k} I_p + \beta_k\right) \quad (23)$$

Mean square error is calculated by Eq. (24). However, O is the obtained output and $\overline{O}$ is expected, and n is the total number of instances.

$$MSE = \frac{1}{n}\sum_{p=1}^{m}(O_p - \overline{O}_p)^2 \quad (24)$$

3.1.2. Sliding mode controller

A sliding mode controller (SMC) is a control system used in engineering and control theory to achieve robust and precise control of dynamic systems. It is particularly effective for controlling systems with uncertainties, disturbances, and nonlinearities. The key concept behind the sliding mode control is to create a sliding surface in the system's state space, drive the system's state trajectory onto this surface and maintain it there.

The basic idea of a sliding mode controller can be as follows:

- Sliding Surface: A sliding surface is a hyper-plane or a sub manifold in the system's state space. It is defined depending on the desired behavior of the system.
- Control Law: The control law is designed to drive the system's state onto the sliding surface and maintain it there. The controller aims to keep the system's trajectory sliding along this surface.
- Sliding Mode: When the system's state lies on the sliding surface, it enters a sliding mode. In this mode, the system's dynamics are simplified, making it easier to control.

Here, Eq. (25) is used to evaluate the error.

$$x_1 = V^{ref}{}_{dc} - V_{dc} = err(n) \quad (25)$$

The Eq. (26) provides the derivative of the estimated error.

$$x_2 = \frac{1}{T}e(n) - err(n-1) \quad (26)$$

Here, T is a time period, and x_1 and x_2 are variables in state space whose expression is Eq. (27)

$$\dot{x} = \begin{bmatrix} \dot{x}_1 \\ \dot{x}_2 \end{bmatrix} = \begin{bmatrix} 0 & 1 \\ 0 & 0 \end{bmatrix}\begin{bmatrix} x_1 \\ x_2 \end{bmatrix} + \begin{bmatrix} 0 \\ -k \end{bmatrix}\mu \quad (27)$$

However, Eq. (28) and (29) each represent the sliding plane's state space equations.

$$s = \begin{bmatrix} C & 1 \end{bmatrix}\begin{bmatrix} x_1 \\ x_2 \end{bmatrix} = Cx_1 + x_2 \quad (28)$$

$$\dot{s} = \begin{bmatrix} C & 1 \end{bmatrix}\begin{bmatrix} \dot{x}_1 \\ \dot{x}_2 \end{bmatrix} = C\dot{x}_1 + \dot{x}_2 \quad (29)$$

According to the power rate law,

$$\dot{s} = -L|s|^{\alpha}\,\mathrm{sgn}(s) \quad (30)$$

Here,

$$\mathrm{sgn}(s) = \begin{Bmatrix} 1 \\ -1 \end{Bmatrix} \; for \; \begin{matrix} s > 0 \\ s < 0 \end{matrix} \quad (31)$$

The Eqs. (32) are used to calculate the μ control law.

$$\mu = \frac{1}{K}\left[Cx_2 + L|s|^{\alpha}\,\mathrm{sgn}(s)\right] \quad (32)$$

The ANN has been trained to produce reference current signals and to maintain constant DLCV. However, to keep the DLCV constant, the reference DLCV ($V^{ref}{}_{dc}$) is compared to the real DLCV (V_{dc}), and the difference error is used as input, withi_{dc} as the target for the neural network, as illustrated in Figure 8. As shown in Figure 9, the load currents (i_{l_a}, i_{l_b}, i_{l_c}) and DC loss component (Δi_{dc}) are treated as input, while the reference currents ($i^{ref}{}_{sh\_a}$, $i^{ref}{}_{sh\_b}$, $i^{ref}{}_{sh\_c}$) are considered as target data. Figure 10 depicts the ANN structure for generating reference signals.

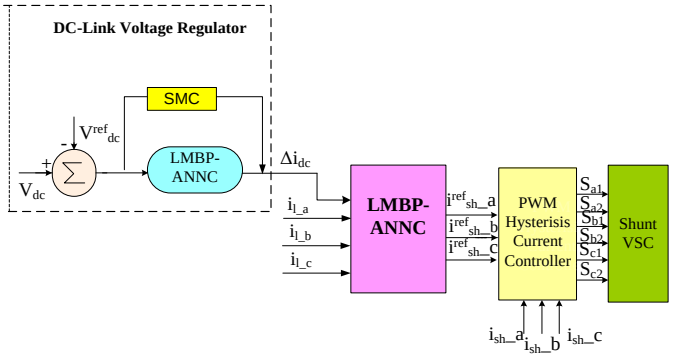

Fig. 8. Shunt VSC controller.

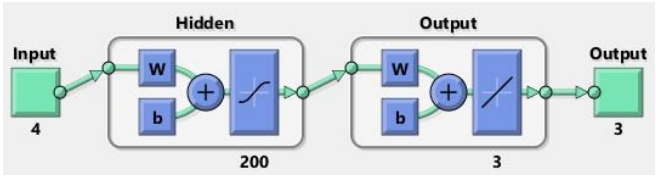

Fig. 9. Structure of ANNC for reference current generation.

3.2. Series VSC

SAPF's primary function is to reduce grid-side voltage aberrations by injecting the appropriate compensating voltage to keep the load voltage constant. Figure 10 depicts the proposed series VSC reference signal-generating technique, and Figure 11 illustrates the construction of an ANN with 200 neurons in the HIL. The supply voltages (V_{s_abc}) are input data to create the reference voltage signals ($V^{ref}_{se\_abc}$), while the reference voltage is considered target data to ANN. PWM is used to create the triggering pulses for series VSC.

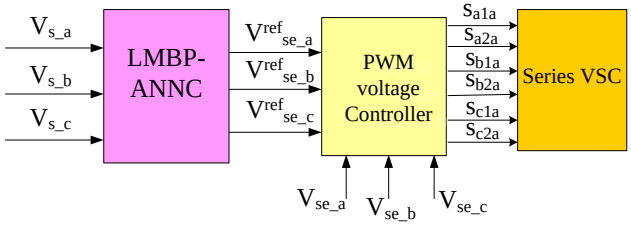

Fig. 10. Series-VSC controller.

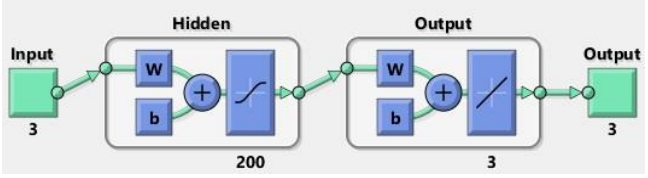

Fig. 11. ANNC for reference voltage signal generation.

4. Simulation and Results

The recommended 5L-UPVBES with ANNC has been developed in Matlab 2016a and executed on an Intel core-i5, 2.67 GHz, 8GB DDR system. Figure 12 depicts the model created using Matlab/ Simulink. In Figure (a) illustrates the 5Level diode clamped VSC model for UPQC, and Figure (b) provides the proposed ANNC control scheme adopted for shunt and series converters. The selected system and the UPQC device parameters chosen are displayed in Table 4. However, two test cases with various permutations of voltage issues like sag, disturbance, swell, balanced and unbalanced loads with constant irradiation (G) and temperature of 25^0c were selected to revel the working of developed ANNC on 5L-UPVBES is given in Table 5. For both cases 1 and 2, the sag in voltage, disturbance, and swell were considered. However, in this work, the reduction of current THD is considered objective, which is obtained by developed ANN for reference signal generation and optimal selection of shunt and series controller parameters for diode clamped 5L-UPQC. Additionally, to show the performance of the proposed ANN, a comparative analysis is carried out with PIC and SMC methods at DLCV balancing. The THD is evaluated by Eq. (33).

$$THD = \frac{\sqrt{(I^2{}_2 + I^2{}_3 + ...I^2{}_n)}}{I_1} \quad (33)$$

Where,

I_n= individual harmonic current distortion values in amps

I_1= individual harmonic current distortion values in amps

I_2= 2nd harmonic current distortion values in amps

The voltage sag/ swell ($V_{sag/swell}$) is evaluated by Eq. (34)

$$V_{sag/swell} = \frac{V_l - V_S}{V_l} = \frac{V_{se}}{V_l} \quad (34)$$

The injected voltage by the series filter is calculated by Eq. (35)

$$V_{se} = V_l - V_S \quad (35)$$

The injected current by the shunt filter is calculated by Eq. (36)

$$i_{sh} = i_i - i_S \quad (36)$$

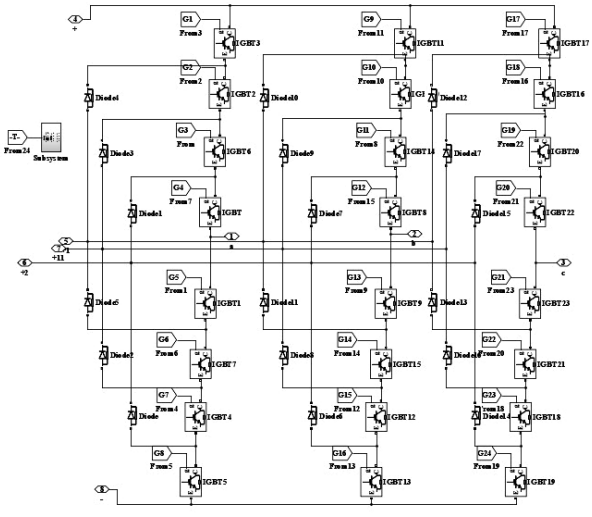

(a) Diode clamped 5-level VSC

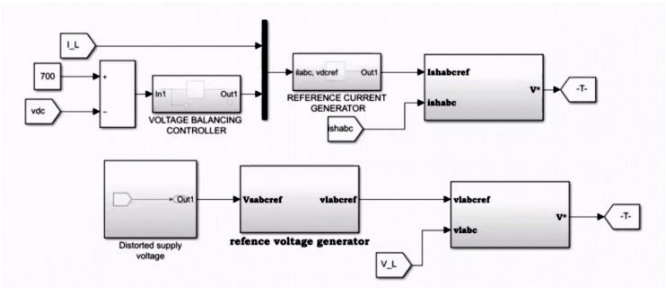

(b) Proposed ANN based reference signal generation scheme

Fig. 12. Simulink model of the proposed system.

Table 4. System and 5L-UPQC parameters

Grid Supply	V_s: 415Volts ;f : 50Hertz; R_s: 0.1ohm ; L_s: 0.15 mH
DC link capacitor & coupling inductors	C_{dc} : 2200μF; L_{se}= 6 mH, L_{sh}=15 mH
Loads	1. Balanced3 Φ load: P_L=3kW, Q_L=0.5 kVAR 2. Un-balanced load: P_{La}=3kW, Q_{La}=9 kVAR; P_{Lb}=4kW, Q_{Lb}=10 kVAR; P_{Lc}=4kW, Q_{Lc}=10kVAR

Table 5. Test Cases studies considered for different loads

Condition	Case1	Case2
Balanced V_S	✓	✓
Source voltage Sag/Swell, disturbance	✓	✓
Current	✓	✓
Constant Irradiation 1000W/m2 and 25^{0}c temperature	✓	✓
THD (both V and I)	✓	✓
Load 1	✓	
Load 2	✓	✓

In case study 1, 30% of sag/ swell occurs, and a disruption in supply voltage occurs over the periods of 0.2 to 0.3 sec, 0.4 to 0.5 sec, and 0.6 to 0.7 sec, as illustrated in Fig 13(a). The established ANN approach effectively detects voltage dips, increases, and disturbances and supplies the necessary compensating voltage via the interface transformer while keeping the load voltage constant. Besides, to exhibit the behavior of the shunt filter with ANNC, Loads 1 and 2 were chosen. From Fig. 13(b) it has been identified that the load current waveform is unbalanced and non-sinusoidal. The developed method suppresses the distortions in the current, with a view of reducing THD to 2.33% and load voltage to 0.23%, which is much less than other techniques and pf enhanced to 0.9845. In addition, it regulates DLCV stable as shown in Fig 13(c) for constant 1000W/ m^2 irradiation and 25^{o}C of constant temperature.

In case 2, similar to case 1, the disturbance is introduced to the 30% of balanced sag and swell. However, the proposed system successfully identifies and eliminates it by injecting the required compensating voltage, as illustrated in Figure 14(a). The load current waveform was sinusoidal but unbalanced, as shown in Figure 14(b), due to unbalanced load 2. However, the developed technique reduces the THD of grid current to 3.78% and load voltage to 0.21%, which is lesser than other techniques, and Pf improved to 0.975. However, the suggested method maintains constant DLCV, as Figure 14 (c) shows.

Table 6 compares the THD of the proposed method with those of other standard techniques like PIC, SMC, ANN and others exits in the literature survey. It exhibits that the proposed method has much lower THD when compared to other techniques. However, Figure 15 exhibits that the proposed method works well during irradiation variation condition, and Figure 16 represent the FFT analysis of the currently proposed system. Finally, Figure 17 exhibits the performance of the proposed method for the power factor enhancement.

Table 6. THD comparison

	Method [Ref]	THD					
		Source Current			Load Voltage		
		Phase-a	Phase-b	Phase-c	Phase-a	Phase-b	Phase-c
Case-1	**Proposed method**	**2.33**	**2.46**	**2.45**	**0.23**	**0.81**	**0.80**
	ANNC	2.65	2.81	2.80	0.37	0.67	0.75
	PIC	2.37	2.15	2.53	4.05	3.54	2.55
	SMC	2.12	2.06	2.18	4.07	4.39	4.01
	2L-UPQC [29]	5.42	5.43	5.61	4.03	3.86	4.04
	3L-UPQC [29]	4.72	4.45	4.86	3.37	3.27	3.36
	5L- UPQC [29]	3.85	4.09	4.40	3.02	2.97	3.03
	2L-UPQC-SRF [29]	5.47	6.07	5.95	4.45	4.76	4.99
	3L-UPQC-SRF [29]	5.55	6.06	4.94	4.22	4.24	4.43

	5L-UPQC-SRF [29]	4.55	5.45	4.32	3.83	3.98	4.22
	ANN [7]	3.72	--	--	--	--	--
	Proposed method	**3.78**	**3.77**	**3.77**	**0.21**	**0.83**	**0.82**
Case-2	ANNC	3.83	3.89	3.90	0.36	0.66	0.75
	PIC	3.86	3.75	4.14	4.05	3.54	2.55
	SMC	3.79	3.71	3.87	2.89	4.12	3.47
	ANN [7]	4.55	--	--	--	--	--

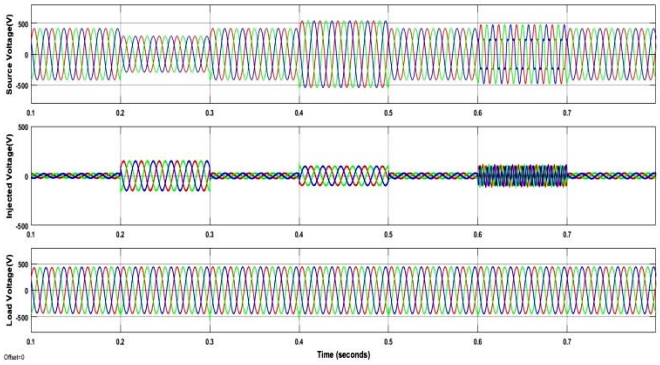

(a) V_S , V_{se} , V_l

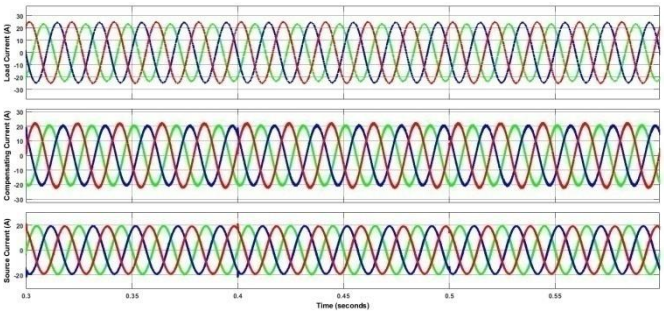

(b) i_l , i_{sh} , i_S

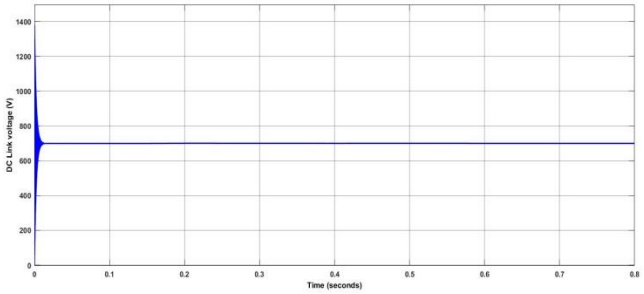

(C) DLCV

Fig. 13. Waveforms of developed method for case-1.

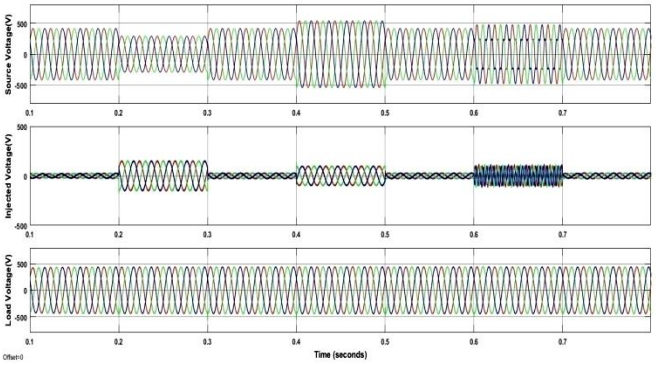

(a) V_S , V_{se} , V_l

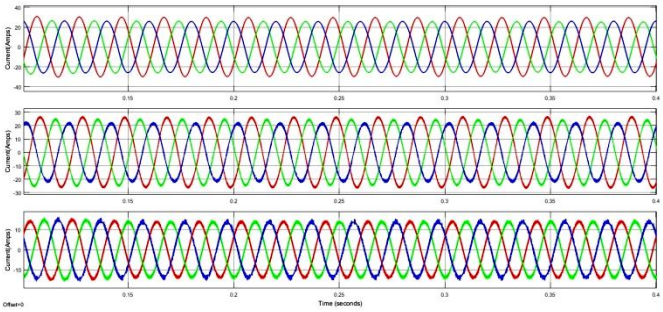

(b) i_l , i_{sh} , i_S

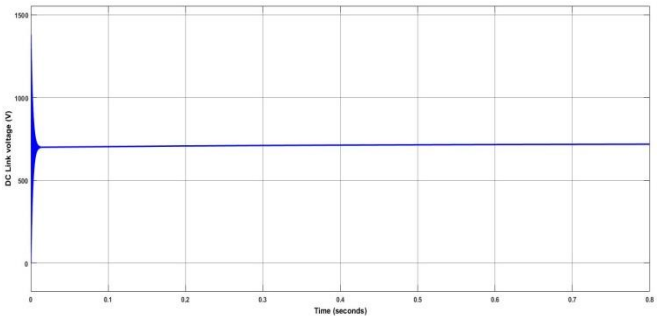

(c) DLCV

Fig. 14. Waveforms of developed method for case-2.

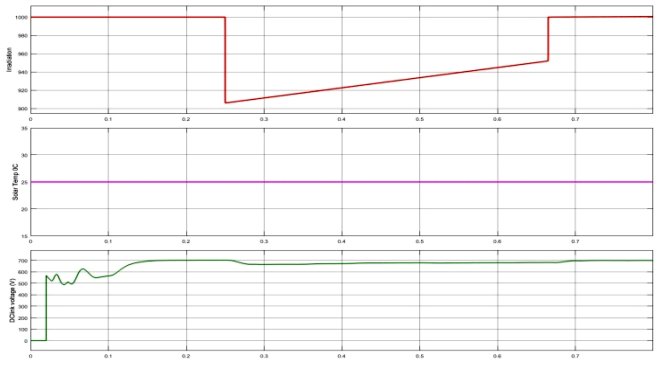

Fig. 15: Constant DLCV with variable irradiation.

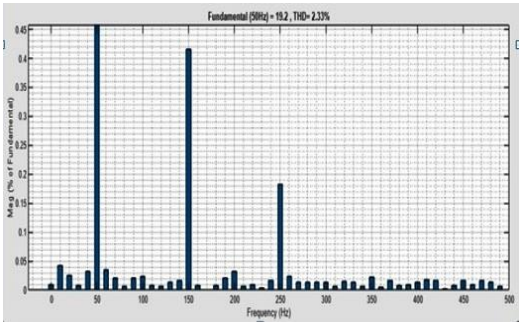

(a) Case-1

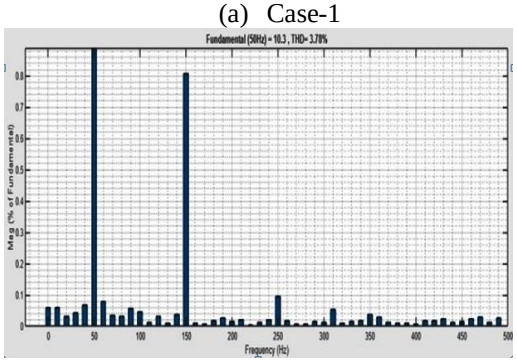

(b) Case-2

Fig. 16. THD spectrum for case studies.

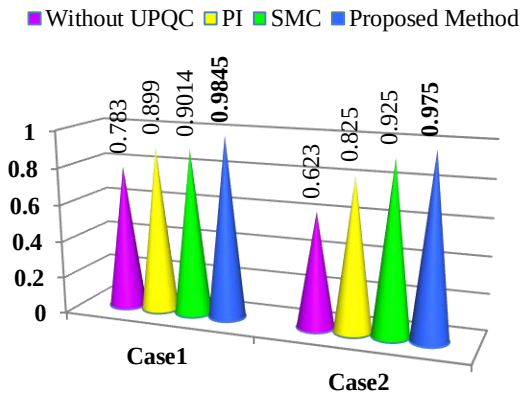

Fig. 17. Comparison of PF.

5. Conclusion

This work proposes an ANNC-based method for a solar battery connected to UPQC. The LMBP-trained ANN controller is presented to produce the required reference signals for shunt series VSC to avoid the traditional abc-dq0-αβ conversions. The hybrid ANN with SMC is adopted for DC link balancing in the Shunt converter. However, the developed 5L-UPVBES maintains constant DLCV during load variations suppresses the source current and load voltage harmonics and improves the current and voltage waveform shape, thereby enhancing power factor and eliminating the fluctuations of supply voltage (disturbance, sag and swell). Here, to show the performance of the proposed scheme, the comparison is done with PIC and SMC controllers for DLCV balancing and other methods available in the literature. Monitoring the results of the two cases shows the developed system provides much lower THD compared to other processes within the acceptable levels. The developed method can be carried out using the ANFIS control scheme in the future.

References

[1] D. Mahdi and G. Gorel, "Design and Control of Three-Phase Power System with Wind Power Using Unified Power Quality Conditioner", Energies 2022, vol. 15, No. 19, pp. 7074, Sep-2022.

[2] A. Mishra, S. R. Das , P. K. Ray , R. K. Mallick, A. Dillip,K. Mishra, "PSO-GWO Optimized Fractional Order PID Based Hybrid Shunt Active Power Filter for Power Quality Improvements", IEEE Access, vol.8, pp. 74497 - 74512, May-2020.

[3] G. Arunsankar, and S. Srinath, "Optimal controller for mitigation of harmonics in hybrid shunt active power filter connected distribution system: An EGOANN technique", Journal of Renewable and Sustainable Energy, vol. 11, No. 2, pp. 025507, April-2019

[4] X. Zhao,X. Chai, X. Guo, A. Waseem, X. Wang and C. Zhang, "Impedance Matching-Based Power Flow Analysis for UPQC in Three-Phase Four-Wire Systems", Energies, vol.14, No. 9, pp. 2702, May-2021

[5] D. Yang , Z. Ma , X. Gao , Z. Ma, E. Cui, "Control Strategy of Integrated Photovoltaic-UPQC System for DC-Bus Voltage Stability and Voltage Sags Compensation", Energies, vol. 12, No. 20, pp. 4009, Oct-2019.

[6] K. Srilakshmi, K. K. Jyothi, G. Kalyani& Y. S.P Goud. "Design of UPQC with Solar PV and Battery Storage Systems for Power Quality Improvement. Cybernetics and Systems: An International Journal", March-2023.

[7] M. A. Mansoor, K. Hasan, M.M. Othman, S. Z. B. M. Noor, and I. Musirin. "Construction and performance investigation of three phase solar PV and battery energy storage system integrated UPQC", IEEE Accesses, vol.8, pp. 103511 – 103538, May-2020.

[8] Y. Hoon, M. A. MohdRadzi, M. Hassan, N.F. Mailah, "Control Algorithms of Shunt Active Power Filter for Harmonics Mitigation: A Review", Energies, vol.10, No.12, PP. 2038, Dec-2017.

[9] T. Chiao Lin, B. Simachew, "Intelligent Tuned Hybrid Power Filter with Fuzzy-PI Control", Energies, vol. 15, No. 12, pp. 4371, June-2022.

[10] O.E Okwakol, Z. Hui Lin, M. Xin, K. Premkumar, Alukaka, "Neural Network Controlled Solar PV Battery Powered Unified Power Quality Conditioner for Grid Connected Operation", Energies, vol. 15, No. 18, PP. 6825, Sep-2022.

[11] K. Sarker, D. Chatterjee & S. K. Goswami, "A modified PV-wind-PEMFCS-based hybrid UPQC system with combined DVR/STATCOM operation by harmonic compensation", International Journal of Modeling and Simulation, vol.41, No.4, pp. 243-255, March 2020.

[12] A. Szromba, "The Unified Power Quality Conditioner Control Method Based on the Equivalent Conductance Signals of the Compensated Load", Energies, vol. 13, No. 23, pp. 6298, Nov-2020.

[13] K. Chandrasekaran, J. Selvaraj, C. Amaladoss, L. Veerapan, "Hybrid renewable energy based smart grid system for reactive power management and voltage profile enhancement using artificial neural network, Energy Sources, Part A: Recovery, Utilization, and Environmental Effects", vol. 43, No. 19, pp. 2419–2442, sep-2022.

[14] B. Aljafari, K. Rameshkumar, V. Indragandhi, S. Rama chandran, "A Novel Single-Phase Shunt Active Power Filter with a Cost Function Based Model Predictive Current Control Technique", Energies, vol.15, No. 13, pp. 4531, Jun-2022.

[15] Y. Hoon, M. A. MohdRadzi, M. A. A. MohdZainuri, M. Zawawi , "Shunt Active Power Filter: A Review on Phase Synchronization Control Techniques", Electronics, vol. 8, No. 7, pp. 791, July-2019.

[16] M. Nicola, C. Nicola, D. Sacerdoțianu and A. Vintilă, "Comparative Performance of UPQC Control System Based on PI-GWO Fractional Order Controllers, and Reinforcement Learning Agent", Electronics,vol. 12, No. 3, pp. 494, Jan-2023.

[17] U.K. Renduchintala, C. Pang, K.M. Tatikonda, L. Yang, "ANFIS-Fuzzy logic based UPQC in interconnected microgrid distribution systems: modeling, simulation and implementation", The Journal of Eng, vol. 2021, No. 1, pp. 6–18, Feb-2021.

[18] Sayed J.A, R. A, Sabha, K. J. Ranjan, "Biogeography based optimization strategy for UPQC PI tuning on full order adaptive observer based control. IET Generation", Transmission & Distribution, vol. 15, No.2 pp. 279-293, Jan-2021.

[19] A. Nafeh , A. Heikal , R. A. El-Sehiemy, W. A.A. Salem, "Intelligent fuzzy-based controllers for voltage stability enhancement of AC-DC micro-grid with D-STATCOM", Alexandria journal of Engineering, vol.61, No. 3, pp. 2260-2293, March-2022.

[20] A. A. Imam, R. Sreerama Kumar, Yusuf A. Al-Turk, "Modeling and Simulation of a PI Controlled Shunt Active Power Filter for Power Quality Enhancement Based on P-Q Theory", Electronics, vol. 9, No. 4, pp. 637, April-2020.

[21] A. Sakthivel, P. Vijayakumar, A. Senthilkumar , L. Lakshminarasimman, S. Paramasivam, "Experimental investigations on ant colony optimized pi control algorithm for shunt active power filter to improve power quality", Control Engineering Practice. vol.42, pp. 153-169, Dec-2015.

[22] K. Srilakshmi, C. Narahari Sujatha, P. Balachandran, L. Mihet-Popa, and N. Udaya Kumar, "Optimal Design of an Artificial Intelligence Controller for Solar-Battery Integrated UPQC in Three Phase Distribution Networks", Sustainability, vol. 14, No. 21, pp. 2-30, Oct-2022.

[23] S. Mahaboob, S. Kumar Ajithan, S. Jayaraman, "Optimal design of shunt active power filter for power quality enhancement using predator-prey based firefly optimization", Swarm and Evolutionary computation, vol. 44, 522-533, (2019).

[24] C. Pazhanimuthu, S. Ramesh, "Grid integration of renewable energy sources (RES) for power quality improvement using adaptive fuzzy logic controller based series hybrid active power filter (SHAPF)", Journal of Intelligent & Fuzzy Systems, vol. 35, No.1, pp. 749–766, July-2018.

[25] Rajesh, P, Shajin, F.H, Umasankar. L, "A Novel Control Scheme for PV/WT/FC/Battery to Power Quality Enhancement in Micro Grid System: A Hybrid Technique", Energy Sources, Part A: Recovery, Utilization, and Environmental Effects 2021, pp. 1-18.

[26] S. Koganti, K.K. Jyothi and S. Salkuti , "Design of Multi-Objective-Based Artificial Intelligence Controller for Wind/Battery-Connected Shunt Active Power Filter, Algorithms, vol. 15, No. 8, pp. 256, 2022, July-2022.

[27] A. Ramadevi ,K. Srilakshmi ,P. Balachandran ,IlhamiColak ,C. Dhanamjayulu ,and Baseem Khan, "Optimal Design and Performance Investigation of Artificial Neural Network Controller for Solar- and Battery-Connected Unified Power Quality Conditioner", International Journal of Energy Research, vol. 2023, PP. 3355124, April-2023.

[28] K. Srilakshmi, N. Srinivas , B. Praveen , J. Ganesh Prasad Reddy, S. Gaddameedhi, N. Valluri, S. Selvarajan, "Design of Soccer League Optimization Based Hybrid Controller for Solar-Battery Integrated UPQC", IEEE Access, vol. 10, pp. 107116-107136, Oct-2022.

[29] S. Vinnakoti, V. Reddy Kota, "Implementation of artificial neural network based controller for a five-level converter based UPQC", Alexandria Engineering Journal, Elsevier, vol.57, No. 3, pp.1475-1488, March-2017.

[30] H. Kenjrawy, C. Makdisie, I. Houssamo, N Mohammed, "New Modulation Technique in Smart Grid Interfaced Multilevel UPQC-PV Controlled via Fuzzy Logic Controller", Electronics, vol.11, No.6, pp. 919, March-2022.

[31] Z. Ming, W. Ru, W. Qiang, Cui Jian, "Control Method for Power Quality Compensation Based on Levenberg-Marquardt Optimized BP Neural

Networks", 2006 CES/IEEE 5th International Power Electronics and Motion Control Conference.

[32] F. Ayadi; I. Colak; I. Garip, H. Bulbul, "Impacts of Renewable Energy Resources in Smart Grid", 8th International Conference on Smart Grid, Paris, pp. 183-188, June 2020.

[33] I. Colak; R. Bayindir, S. Sagiroglu, "The Effects of the Smart Grid System on the National Grids", 8th International Conference on Smart Grid, Paris, pp. 122-126, June 2020.

[34] S. Jaber, A. M. Shakir, "Design and Simulation of a Boost-Microinverter for Optimized Photovoltaic System Performance", International Journal of Smart Grid, vol. 5, No. 2, pp. 1-9, June 2021.

[35] S. S. Dash, "Tutorial 1: Opportunities and challenges of integrating renewable energy sources in smart" 6th International Conference on Renewable Energy Research and Applications , San Diego, CA, USA, 5-8 Nov. 2017.

[36] M. Tsai, C. Chu, W. Chen, "Implementation of a Serial AC/DC Converter with Modular Control Technology", 7th International Conference on Renewable Energy Research and Applications, Paris, France, pp. 245-250, Oct. 2018.

[37] A. Belkaid, I. Colak, K. Kayisli, R. Bayindir, "Improving PV System Performance Using High Efficiency Fuzzy Logic Control", 8th International Conference on Smart Grid, Paris, pp.152-156, June 2020.

[38] K. Srilakshmi, K. Kondreddi, N. V. Gowri, V. Ramprasad, "Optimal design of hybrid green energy powered reduced switch converter based shunt active power filter using horse herd algorithm, Sci Rep, vol. 14, pp. 20447, Sep2024.

[39] K. Srilakshmi, D. Santosh, A. Ramadevi, "Development of renewable energy fed three-level hybrid active filter for EV charging station load using Jaya grey wolf optimization", Sci Rep, vol. 14, pp. 4429, Feb2024.

[40] K.Srilakshmi, K. Amit, K. Kondreddi, "Design of solar and energy storage systems fed reduced switch multilevel converter with flower pollination optimization, Journal of Energy Storage, vol. 99, Part A,pp. 113324, Oct-2024.

[41] K. Srilakshmi, A. Ramadevi, J. G. P. Reddy, K. K. Jyothi, K. krishnaveni, P. K. Balachandran, & I. Colak, "A New Control Scheme for Wind/Battery Fed UPQC for the Power Quality Enhancement: A Hybrid Technique", IETE Journal of Research, Vol. 70, no. 11, pp. 8184–8191, Jul 2024.